High Speed Release Dynamics of Microfabricated Hooks for Fiber and Wire Grasping

Jasmin Beharic[1] and Cindy Harnett[2] *Member, IEEE*

***Abstract*— This paper reports on the steps that happen after the release of strained microhooks from silicon substrates. The application is automated microassembly of electronic circuits using clips that grasp microscale (< 200 micron diameter) conductive fibers. We developed an integrated, photoresist-based thermal release structure that allows the first direct observations of the release process outside the etch chamber. High speed camera video (4200 frames/s) shows the cantilevers release in an order determined by thermal diffusion, with groups of ~1200 micron long cantilevers releasable at 100 Hz. Side-view video is analyzed to show that the height of the graspable region is approximately half the hook length.**

***Keywords*— Microassembly, contacts, electronic packaging, strain engineering.**

I. Introduction

Microscale devices such as integrated circuits (ICs) are usually assembled into electronic packages by wirebonding. This permanently-bonded wire makes a 3D electrical circuit from IC pad to chip package, and ultimately to a circuit board with wires that deliver power and communication to the IC. In this work, we apply thin-film microfabrication to integrate the bonding wires into the microscale device itself, using internal stress to produce a 3D hook that clips itself directly and reversibly onto a wire when thermally released from the silicon wafer.

The larger goal is to expand the reach of pick-and-place assembly and other heterogeneous assembly methods such as microtransfer printing [1–5] to new materials and substrates. Advantages of this non-adhesive method include the ability to remove the connection by differential thermal expansion [6], to passively accommodate imprecise alignment with built-in spring forces, to mechanically bind to highly porous structures such as wire meshes, and to make connections between materials that are difficult to solder.

Our previous work explored the electronic properties of such connections [7]. Now we add a current-driven thermal release method for individual devices. This paper investigates the mechanical properties of the resulting microhooks, the high-speed events that happen when the hooks are released from the surface, and the implications for automated assembly of circuits onto wires, fabrics, and meshes.

II. Methods

The method described in this section creates microhook arrays with metal on the inside and an insulating oxide layer on the outside. For mechanical testing purposes, we also created individual cantilevers, each connected to a square anchor pad. Because the pad is significantly wider than the cantilever, it does not get fully undercut and keeps the microhook anchored to the wafer surface. In further applications such as chip transfer, entire device removal could use sacrificial layers and etch holes for full release.

A. Thermal Release of Strain Engineered Micro Hooks

The process shown in Fig. 1 uses a metal film over a thermally grown, compressively-stressed SiO_2 layer on silicon to introduce a strain mismatch. When released from the wafer, the structure curls upward, reaching a strain energy minimizing radius in the range of 50-200 microns depending on the layer thicknesses and elastic moduli [8–10]. In our previous work, such structures were released using XeF_2 vapor etching to undercut the silicon. In the current work, the same etching process is carried out, but now we introduce a set of polymer tethers at the end of the device. These features keep devices planar until the tethers are melted by activating a built-in heating wire. This separation of vapor etching from untethering allows each device to be individually released after alignment to wires. The wires don't need to fit into the etch chamber or be chemically compatible with XeF_2, and tether release in open air for the first time allows a high speed camera to focus on the hooks at the moment of release.

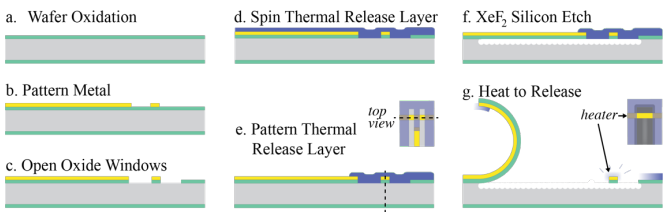

Figure 1: Silicon wafer fabrication steps for fast release of microfabricated strained cantilevers by melting a polymer tether using an integrated heating trace. Fig 1e cross section runs through heater trace.

The microhook layout parameters are listed in Table 1. In this work, the metal for both microhooks and heater traces is 130 nm platinum with a 40 nm titanium adhesion layer, and the polymer tethers are made from Shipley 1827 photoresist (Rohm and Haas, Inc.) spun at 4000 rpm.

Figure 2 shows a heater trace and microhook tips running under a row of photoresist polymer tethers, which appear translucent in optical images. During activation by Joule heating, the estimated temperature of the heater trace is

*Research supported by NSF Award 2309482.

J. Beharic and C. Harnett are with the University of Louisville, Louisville, KY 40208 USA (corresponding author e-mail: c0harn01@louisville.edu).

approximately 200 °C, sufficient to reflow photoresist films in this family [11].

TABLE I. MICROHOOK DESIGN PARAMETERS

Parameter	*Value*	*Unit*
microhook width	10	micron
microhook length	900-1200	micron
oxide thickness	500	nm
total metal thickness	170	nm
polymer tether thickness	2.7	micron
heater trace length	430	micron
heater trace width	10	micron

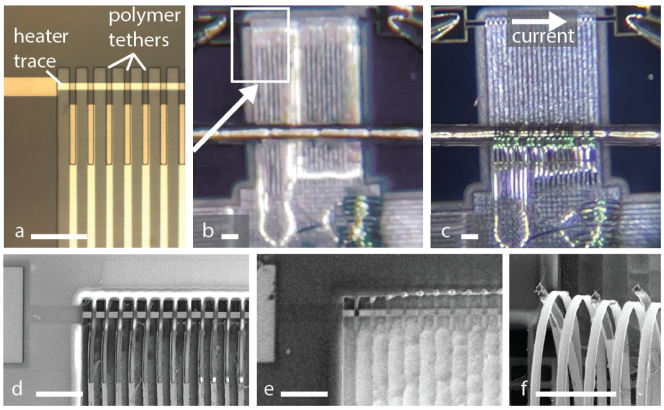

Figure 2: All scale bars 100 micron. a-c: Optical microscope images of a: a row of tethers before silicon undercutting (step e in Fig. 1 process diagram), b: microhooks undercut and aligned to a wire, c: hooks released onto the wire after supplying 15 mA from probe tips. d-f: Electron micrographs showing d: an undercut tether region (step f in Fig.1), e: a tether region after release, and f: tether residue visible on the inside of curled hook tips without a wire present.

In the example of Figure 2b-c, a group of 21 parallel microhooks is released onto a 150 micron diameter conductive thread (single strand 3981 tinned Cu, Karl Grimm GmbH, Germany) that has been manually aligned over the microhook region for grasping. Polymer residue (fig. 2f) insulates the tips of the released microhooks, but the rest of the beam is uninsulated for electrical contact with the wire. In the following sections, we focus on understanding the speed, sequence, and geometry of the release process without wires in place.

B. Observing Mechanical Properties of Tethers

In order to use the hooks as both electronic and mechanical connectors, the thin film (~1 micron) hooks need to be strong enough and numerous enough to withstand loads during the intended application. Force-vs-deflection characteristics were investigated by scanning a profilometer stylus (Dektak profilometer, Veeco Inc., USA) along curled 10 micron wide test structures at a force of 1 mgf (~10 mN) and speed of 50 microns per second, and measuring the deflection as the hook was unrolled and flattened out by the stylus. These test beams had the same dimensions as the grippers, but instead of an array they were individual beams each attached to a large square pad. The hook resumed its original curled shape after the force was removed. The result was a force-vs-deflection curve for constant force applied at points along the beam.

C. Observing Tether Release Sequence

To observe the release sequence in detail, we used a high speed camera (Phantom V310, 4200 frames per second) in top and side views. Figure 3 shows a microhook chip ready for release, with thermal release traces for three separate sets of microhooks wirebonded to a carrier circuit. Samples were placed on a stage in front of a high speed camera for observation while the heater trace was supplied with current from a sourcemeter.

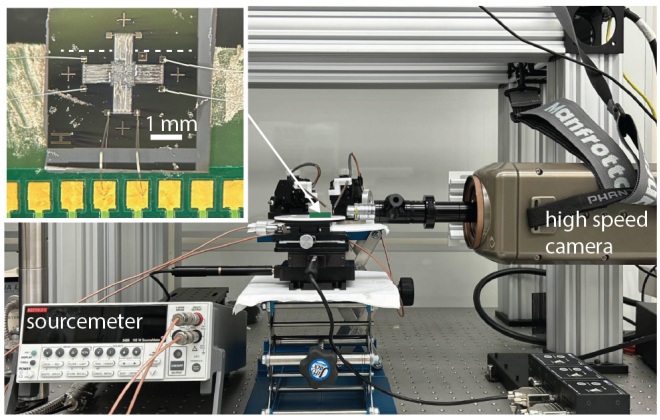

Figure 3: Setup for high speed camera observations of thermal release of beams from chip (inset), driven by current from a sourcemeter. Dashed line shows the position of the wire in Fig. 2b,c; subsequent experiments do not involve wires.

III. RESULTS AND DISCUSSION

A. Thermal Release Characteristics and Outcome

Thermal release was observed to require 15 mA. Because heater trace resistances were approximately 130 ohms including contact resistance, these currents were driven by applying approximately 2 V. Fig. 2b shows the grippers before this process and Fig 2c shows the outcome.

The design parameters in Table 1 created hooks with an approximately 100 micron radius of curvature. The wire running horizontally across the layout prevented them from forming a fully circular cross-section in Fig. 2c and the stored strain energy helped them maintain contact on the wire at the outside of the loop. This springlike behavior is the premise for electrical contact even when the microhook radius of curvature is larger than the radius of the wire or fiber. Because an opposing force is necessary to keep the contacts under tension, the method is designed for a device that has two or more contact terminals with microhooks making contact to wires on each side.

B. Mechanical Properties

Constant-force profilometry results for four different test samples are overlapped in Fig. 4, with final probe height varying between 12 and 20 micron stemming from the high

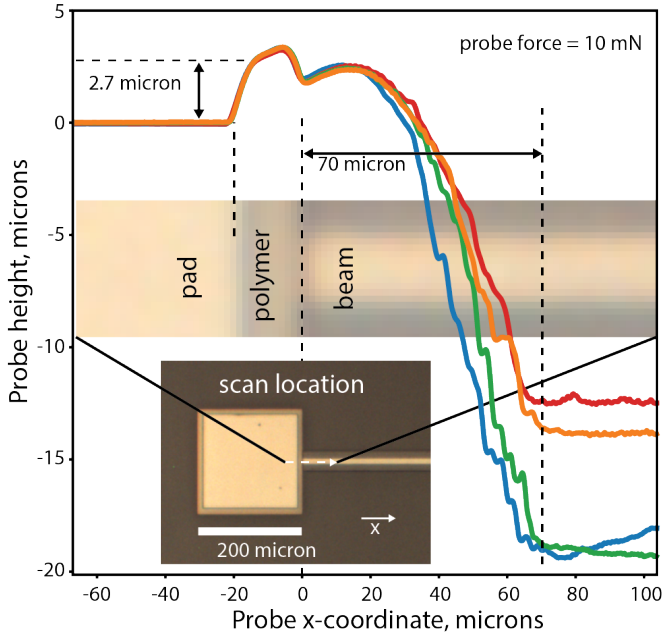

Figure 4: A 10 mN probe was scanned along four different released, curled 10 micron wide mechanical test structures made on the same wafer as the microhooks and with the same beam width. At 70 microns from the pad, the probe is able to push the microhook to the bottom of the etched silicon region.

sensitivity of the XeF_2 etch rate to the amount of exposed silicon nearby. Over this range of etch depths, the 10 mN force was able to collapse the microhook to the bottom of the channel at a distance of approximately 70 micron from the supporting point. This distance is on the order of the microhook radius of curvature and the radius of the wire in Fig. 2b,c. To withstand forces of greater than 10 mN in such wire-gripping applications, multiple parallel microhooks, potting in a stronger material after assembly, or thicker microhook materials should therefore be used. In such cases, additional or thicker tethers than the 2.7 micron thick photoresist may be needed to keep the microhooks planar before transfer.

C. Dynamic Behavior

The dynamic behavior of the beams was captured using the high speed camera in top view and side view modes. Fig. 5 shows selected top view frames during thermal release of a 19 beam, 1200 micron long microhook array by delivering current from probe tips to the heater. In Fig. 5, the beams can be seen releasing first near the more thermally isolated center of the wire (Beam 15), after which neighboring beams begin to release. The right side in Fig. 5 is missing two beams (20 and 21), giving it more thermal isolation than the left and making it more likely to release first.

Side view measurements were carried out using the wirebonded 900-micron beam length array shown in the inset image of Fig. 3. For these experiments, the goal was to determine the swept region of the hooks, guiding placement of fibers and wires for gripping. The top row of Fig. 6 (Fig. 6 a-e) shows this release process at the same frame timings as the other device released in the top-view Fig. 5. Because the camera's depth of field was too limited to focus on all beams in the side view, the second row (Fig. 6 f-j) shows pixel value differences *vs.* the t=0 frame to highlight changes during release. The bottom row has overlays circling the swept regions in the contrast-enhanced images from the center row. For this beam length, the combined swept region in Fig. 6k shows that it will be important to keep wires and fibers within 0.5 mm of the surface for any chance at grasping. Fibers should also be in front of the beam attachment point by less than 0.6 mm (to the right of the wirebond in Fig. 6), conditions satisfied by the grasped fiber in Fig. 2. The camera's frame rate was too low to capture beams before 0.47 ms (Fig. 6l) where they are still close to the surface. However, if the wire is too far toward the end of the beam, the hook does not have enough length to grasp it, so these regions aren't included in the graspable region.

Because multiple beams are likely to be required for mechanical strength, and mandatory for multi-terminal devices, the detailed release sequence for multiple beams and its overall timeframe are of interest for electronic packaging applications. Beam tip trajectories (Fig. 7) were extracted from the top-view video of Fig. 5 to further examine the sequence and settling time. In Fig. 7, which spans less than 5 ms, the blue line representing Beam 1 does not descend because the stuck beam at the left of Fig. 5e takes 21 ms to release, possibly due to better heatsinking near the end of the array (note greater disruption at the center of the heater in Fig. 2e compared to the end). After the rightmost group of beams in Fig. 5 detaches, the process continues toward the left side

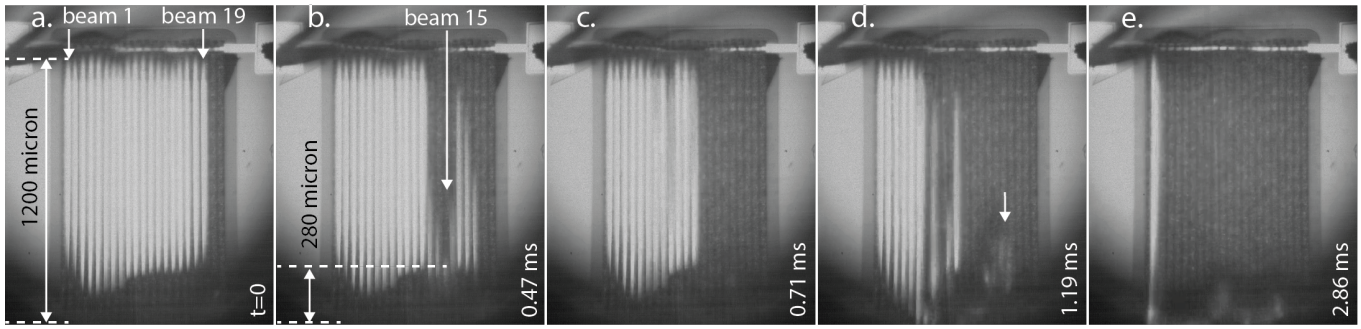

Figure 5: a. Tips of Beams 1 through 19 are at 1200 micron y-coordinate before supplying 15 mA current through the horizontal wire across the tethers. b. At 0.47 ms, beam 15 is the first to release, with a tip y-coordinate of 280 microns. c. The group of beams to the right is released. d. More beams release and previously released beams come into view again (arrow), oscillating at approximately 1 kHz before coming to rest. e. All but Beam 1 are released in < 3 ms, with the final beam eventually releasing at 21 ms.

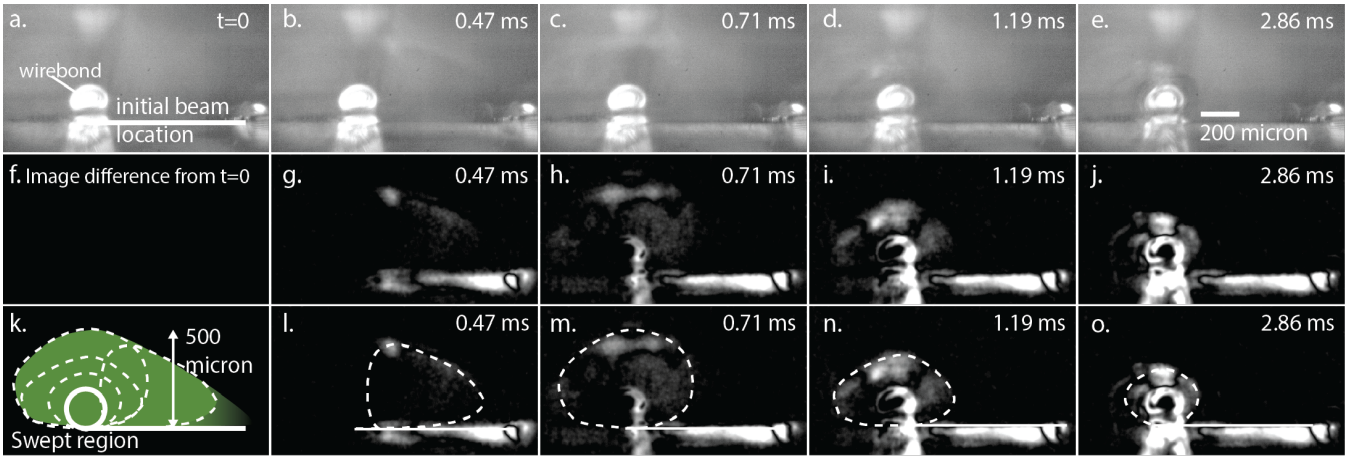

Figure 6: Top row (a-e): side view of 900 micron length beam release with tethers at the right side of the image, and the beam anchoring point aligned with the visible wirebond in the background. 200 micron scale bar in figure 6e applies to all figure parts. Middle (f-j): Images from the top row are differenced from t=0 to show changes. Notable features are scattered light from beams moving above the surface and increased scattering from etched silicon at the surface where beams have been released. Bottom: (k) combined and (l-o) single-frame beam path regions are traced over the differenced images from f-j.

of Fig. 5 in nearly perfect order. In both top-view and side-view video, the beams were observed to oscillate before settling. For example, beams that disappeared at the bottom of Fig. 5c reappeared in Figure 5d and then went off camera again in Fig. 5e. The corresponding frames of the side view video showed a horizontal rocking motion of the circular loops, indicating the loops were partially uncurling and recurling before settling. To study the pattern more quantitatively, we time-shifted the trajectory data from Fig. 7a to align the individual beams' release times. This aligned data in Fig. 7b shows several beams undergoing a damped oscillation with a frequency in the 1 kHz range.

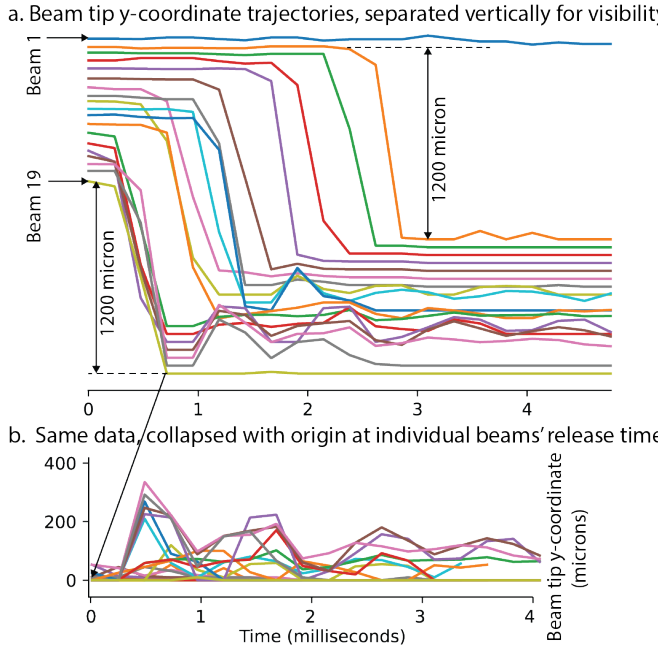

Figure 7 a: Beam tip y-coordinate trajectories obtained from the video frames and coordinate system described in top-view Fig. 5. b: Trajectory data aligned to put each beam's release time at the origin. Here, a y-coordinate of 0 means the beam tip is at the bottom of Fig 5, where y=1200 micron is the unreleased position.

Beam tip y-coordinate minima, indicating a beam fully released and curled towards the bottom of the images in Fig. 5, are separated by approximately 1 ms. They are interleaved with maxima indicating a beam partially uncurled back towards the tether region.

Aside from Beam 1, all the beams were released in < 3 ms and came to rest after another 7.5 ms. This 10 ms (100 Hz) release duration means the throughput of automated transfer is more likely to be limited by feature alignment and stage motion than by the timescale of thermal release.

II. Conclusions And Future Work

Transfer of electronic devices from donor wafers for heterogeneous assembly or for microrobotics applications [12] depends on fast, reliable establishment of electrical and mechanical contact. This work further develops our microhook-based contact method by adding integrated thermal release, showing a potential 100 Hz transfer rate. Optimizing the geometry and materials of the heater traces and tethers could speed up release by carefully controlling the local thermal environment.

Our previous work showed that small differences in feature width were highly reliable in driving repeatable and complex release sequences for strained microbeams released from surfaces during etching [9], but real-time implementation was limited to the etch chamber. Fine-tuning the ability to sequence one-time motion on short timescales using stored mechanical energy may have other applications besides electronic packaging.

Another distinguishing feature of our electronically driven release method is the potential for individual device transfer from a wafer using an automated probe station, where most adhesion-based methods transfer groups or entire wafers of devices.

Application-oriented experiments include further study of how the electrical contact resistance between wire and device develops during grasping, optimizing the number of redundant microhooks necessary for reliable electrical and mechanical contact, and further investigation of the microhooks' mechanical limits using push-off/pull-off tests.

ACKNOWLEDGMENT

This work was supported by NSF Award 2309482. We thank the University of Louisville MNTC cleanroom facility and Michael D. Martin for wirebonding.

REFERENCES

[1] A. Carlson, A.M. Bowen, Y. Huang, R.G. Nuzzo, J.A. Rogers, Transfer printing techniques for materials assembly and micro/nanodevice fabrication, Adv. Mater. 24 (2012) 5284–5318. https://doi.org/10.1002/adma.201201386.

[2] C.A. Bower, M. Meitl, D. Kneeburg, Micro-Transfer-Printing: Heterogeneous integration of microscale semiconductor devices using elastomer stamps, in: SENSORS, 2014 IEEE, ieeexplore.ieee.org, 2014: pp. 2111–2113. https://doi.org/10.1109/ICSENS.2014.6985454.

[3] L. Zhang, C. Zhang, Z. Tan, J. Tang, C. Yao, B. Hao, Research Progress of Microtransfer Printing Technology for Flexible Electronic Integrated Manufacturing, Micromachines (Basel) 12 (2021). https://doi.org/10.3390/mi12111358.

[4] Furong Chen, Jing Bian, Jinlong Hu, Ningning Sun, Biao Yang, Hong Ling, Haiyang Yu, Kaixin Wang, Mengxin Gai, Yuhang Ma and YongAn Huang, Mass transfer techniques for large -scale and high -density microLED arrays, International Journal of Extreme Manufacturing (2022). https://doi.org/10.1088/2631-7990/ac92ee.

[5] R. Saeidpourazar, M.D. Sangid, J.A. Rogers, P.M. Ferreira, A prototype printer for laser driven micro-transfer printing, J. Manuf. Process. 14 (2012) 416–424. https://doi.org/10.1016/j.jmapro.2012.09.014.

[6] M.S. Islam, S. Challa, M.H. Yacin, S.S. Vankayala, N. Song, D. Wei, J. Beharic, C.K. Harnett, Thermally driven MEMS fiber-grippers, Journal of Micro and Bio Robotics (2023). https://doi.org/10.1007/s12213-023-00161-w.

[7] N. Song, D. Wei, C.K. Harnett, Powering Wire-Mesh Circuits through MEMS Fiber-Grippers, in: 2023 IEEE International Conference on Flexible and Printable Sensors and Systems (FLEPS), 2023: pp. 1–4. https://doi.org/10.1109/FLEPS57599.2023.10220225.

[8] O.G. Schmidt, K. Eberl, Nanotechnology. Thin solid films roll up into nanotubes, Nature 410 (2001) 168. https://doi.org/10.1038/35065525.

[9] E. Moiseeva, Y.M. Senousy, S. McNamara, C.K. Harnett, Single-mask microfabrication of three-dimensional objects from strained bimorphs, J. Micromech. Microeng. 17 (2007) N63. https://iopscience.iop.org/article/10.1088/0960-1317/17/9/N01/meta.

[10] J. Rogers, Y. Huang, O.G. Schmidt, D.H. Gracias, Origami MEMS and NEMS, MRS Bull. 41 (2016) 123–129. https://doi.org/10.1557/mrs.2016.2.

[11] C.D. James, R. Davis, M. Meyer, A. Turner, S. Turner, G. Withers, L. Kam, G. Banker, H. Craighead, M. Isaacson, J. Turner, W. Shain, Aligned microcontact printing of micrometer-scale poly-L-lysine structures for controlled growth of cultured neurons on planar microelectrode arrays, IEEE Trans. Biomed. Eng. 47 (2000) 17–21. https://doi.org/10.1109/10.817614.

[12] S. Challa, M.S. Islam, C.K. Harnett, Fiber-Crawling Microrobots, in: 2019 International Conference on Manipulation, Automation and Robotics at Small Scales (MARSS), 2019: pp. 1–6. https://doi.org/10.1109/MARSS.2019.8860986.